International Journal of Pharmaceutics 426 (2012) 116–131

Contents lists available at SciVerse ScienceDirect

International Journal of Pharmaceutics

journal homepage: www.elsevier.com/locate/ijpharm

Instrumented roll technology for the design space development of roller compaction process

Vishwas V. Nesarikar[a,*], Nipa Vatsaraj[a], Chandrakant Patel[a], William Early[a], Preetanshu Pandey[a], Omar Sprockel[a], Zhihui Gao[a], Robert Jerzewski[a], Ronald Miller[b], Michael Levin[c]

[a] Drug Product Science and Technology, Bristol-Myers Squibb, 1 Squibb Drive, New Brunswick, NJ 08901, USA
[b] Miller Pharmaceutical Technology, 16 Crown Ridge Road, Travelers Rest, SC 29690, USA
[c] Milev Pharmaceutical Technology Consulting, 27 Moran Road, West Orange, NJ 07052, USA

ARTICLE INFO

Article history:
Received 14 July 2011
Received in revised form 10 January 2012
Accepted 15 January 2012
Available online 25 January 2012

Keywords:
Roller compaction
Instrumented roll
Process design space
Ribbon normal stress
Ribbon density
Vacuum de-aeration
Roll gap

ABSTRACT

Instrumented roll technology on Alexanderwerk® WP120 roller compactor was developed and utilized successfully for the measurement of normal stress on ribbon during the process. The effects of process parameters such as roll speed (4–12 rpm), feed screw speed (19–53 rpm), and hydraulic roll pressure (40–70 bar) on normal stress and ribbon density were studied using placebo and active pre–blends. The placebo blend consisted of 1:1 ratio of microcrystalline cellulose PH102 and anhydrous lactose with sodium croscarmellose, colloidal silicon dioxide, and magnesium stearate. The active pre-blends were prepared using various combinations of one active ingredient (3–17%, w/w) and lubricant (0.1–0.9%, w/w) levels with remaining excipients same as placebo.

Three force transducers (load cells) were installed linearly along the width of the roll, equidistant from each other with one transducer located in the center. Normal stress values recorded by side sensors and were lower than normal stress values recorded by middle sensor and showed greater variability than middle sensor. Normal stress was found to be directly proportional to hydraulic pressure and inversely to screw to roll speed ratio. For active pre-blends, normal stress was also a function of compressibility. For placebo pre-blends, ribbon density increased as normal stress increased. For active pre-blends, in addition to normal stress, ribbon density was also a function of gap.

Models developed using placebo were found to predict ribbon densities of active blends with good accuracy and the prediction error decreased as the drug concentration of active blend decreased. Effective angle of internal friction and compressibility properties of active pre blend may be used as key indicators for predicting ribbon densities of active blend using placebo ribbon density model. Feasibility of on-line prediction of ribbon density during roller compaction was demonstrated using porosity–pressure data of pre-blend and normal stress measurements. Effect of vacuum to de-aerate pre blend prior to entering the nip zone was studied. Varying levels of vacuum for de-aeration of placebo pre blend did not affect the normal stress values. However, turning off vacuum completely caused an increase in normal stress with subsequent decrease in gap.

Use of instrumented roll demonstrated potential to reduce the number of DOE runs by enhancing fundamental understanding of relationship between normal stress on ribbon and process parameters.

1. Introduction

Roller compaction is a dry granulation process used to convert powder blends into free flowing agglomerates. Roller compaction enhances flow properties and improves content uniformity. There are two ways in which the powder is typically fed through the rollers – either by gravity or by means of a feed screw. The powder blend is passed through counter-rotating rolls to form a 'ribbons' or 'flakes' which are subsequently milled to form granules. These milled granules are then blended with extragranular excipients and compressed into tablets. It is a preferred granulation process for blends containing moisture sensitive drug substance(s) that cannot be compressed directly. One of the disadvantages of using roller compaction is the loss of reworkability of the material as it passes the rolls and its effect on the final blend compactability (He et al., 2007).

One of the most important characteristic of the ribbons coming out of a roller compactor is its solid fraction. Solid fraction is defined as the ratio of apparent or envelope density of a sample to the true density of the material. Solid fraction increases as the

* Corresponding author. Tel.: +1 732 227 6430.
E-mail address: vishwas.nesarikar@bms.com (V.V. Nesarikar).

0378-5173/$ – see front matter © 2012 Elsevier B.V. All rights reserved.
doi:10.1016/j.ijpharm.2012.01.032

powder gets compacted and depends on several processing factors including hydraulic roll pressure, screw speed to roll speed ratio and gap. Mechanical properties such as tensile strength, hardness and elasticity of compacted powders depend on the solid fraction. By maintaining comparable ribbon solid fractions across different scales it is expected to achieve similar tensile strengths and subsequently similar particle size distribution when milled under same conditions (Zinchuk et al., 2004).

For scale-up or transfer of unit operations such as tablet compression, relationship between solid fraction of tablets and normal pressure is utilized to achieve the desired solid fraction. Modern tablet presses are equipped with normal force measurements during formation of tablets that facilitate scale up or transfer of tablet compression. This is typically not the case for a roller compactor where such force or pressure sensors do not come standard with the equipment, making scale-up of roller compactor more challenging.

A few researchers have explored experimental measurements of normal stress applied by the rotating roll onto ribbon. Bindhumadhavan et al. (2005) used a gravity fed laboratory scale roller compactor equipped with a piezoelectric pressure transducer to test a theoretical model developed by Johanson (1965). Their research findings showed that for microcrystalline cellulose grade Avicel PH102, measured pressure profiles in the nip region were comparable to values calculated by model. They indicated that the major weakness of the model is the need for accurate estimation of nip pressure which dictates the complete pressure profile.

Moguelez-Moran et al. (2008) used similar instrumented laboratory scale roller compactor to study the effect of lubrication on ribbon density distribution. They showed that density variation across ribbon width was lower for lubricated powder blend compared to un-lubricated powder blend. They also characterized the angle formed when powder is drawn into the rolls and found that sharper angle results in a more heterogeneous ribbon. This was a drag angle defined as projected angle of powder boundary on roll surface as determined by an image processing package. This work was also done on a gravity-fed roller compactor. Meyer et al. (2005) used an instrumented roller compactor with vertical screw feeder to determine the effects of process parameters on the local normal and shear stress distribution. Their work primarily focused on maximum normal stress and ribbon density as a function of process parameters. Their research findings showed that compact density was primarily determined by the maximum normal stress and was linearly related to total roll force and roll gap.

Gravity fed systems are not preferred for commercial scale pharmaceutical manufacturing due to flow challenges and throughput requirements. Therefore, vertical and horizontal feed screw systems are the preferred feeding mechanisms for commercial manufacturing equipment. To authors' knowledge, there is no published work using instrumented roll with horizontal feed screw mechanism, other than the work reported by Guigon and Simon (2003). Their research work focused on variation of local pressure in the feeding zone and its effect on compact density and strength.

In the current work, an instrumented roll on Alexanderwerks® WP120 roller compactor was used for roller compaction of placebo pre-blend and active pre-blends. The placebo formulation consisted of 1:1 ratio of microcrystalline cellulose PH102 and anhydrous lactose with sodium croscarmellose, colloidal silicon dioxide, and magnesium stearate.

Active pre-blends were assumed to represent low drug load formulations. The active pre-blends were prepared using various combinations of one active ingredient (3–17%, w/w) and lubricant (0.1–0.9%, w/w) concentrations with remaining composition made up of same ingredients as placebo pre–blend. The ratio of microcrystalline cellulose PH102 and anhydrous lactose was maintained at 1:1 for all active pre-blends. The placebo pre-blend and active pre-blends were roller compacted at various combinations of process parameters such as roll speed, feed screw speed, and hydraulic roll pressure, the levels determined by a statistical design.

The main aim of the this study was to illustrate the development of statistical models using placebo pre-blend to (1) express ribbon density as a function of maximum normal stress and gap in order to remove machine specific parameter dependence, (2) express maximum normal stress and gap as a function of roll speed, feed screw speed, and hydraulic roll pressure, (3) evaluate application of models developed using placebo for the prediction of ribbon density and process design space of low drug load formulations, (4) evaluate effects of blend properties (e.g. compressibility) on normal stress measurements by varying drug and lubricant concentrations.

This work also illustrates the feasibility of on-line prediction of average ribbon density using pre-blend compaction data (i.e. solid fraction vs. normal pressure) and normal stress data on ribbon collected by the instrumented roll.

Vacuum de-aeration is important during roller compaction to reduce pre-blend leak that occurs due to powder slippage between individual particles and roll surface. Vacuum de-aeration affects the flow of pre-blend into nip zone. Therefore, effect of vacuum level on normal stress measurements was also studied. Fig. 1 shows the schematic of the overall approach described in this paper.

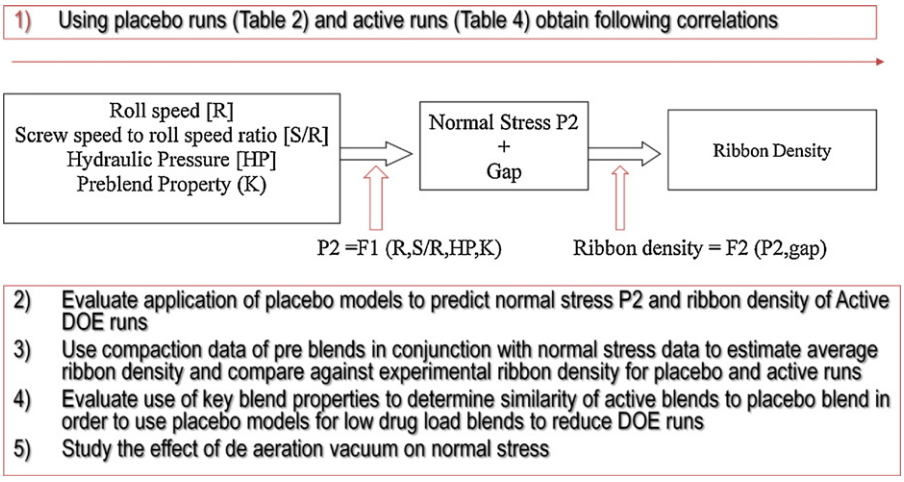

Fig. 1. Overall summary of experimental approach described in this manuscript.

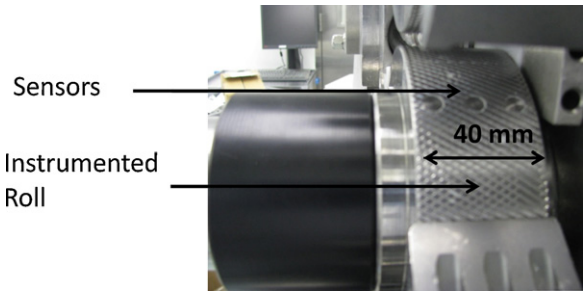

Fig. 2. Instrumented roll installed on Alexanderwerks® WP120 roller compactor.

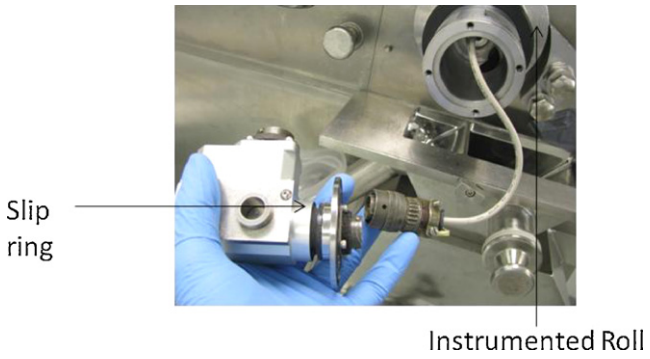

Fig. 3. Slip ring assembly of instrumented roll.

2. Experimental

2.1. Instrumentation

The instrumented roll used in this work was manufactured by Metropolitan Computing Corporation (East Hanover, New Jersey). The instrumented roll was installed on the bottom shaft of an Alexanderwerk® WP120 roller compactor. Both upper and lower rolls used in this study were 'knurled' rolls. Commercial force transducers (load cells) for measuring normal pressure on the roll in the nip area were installed on the 120 mm 'knurled' roll. The pressure is transmitted to the load cells through probes. Three subminiature load cells (222 N capacity, 0.1% FS repeatability), including custom-built amplifier and signal conditioner, were installed on the roll. The original roll was machined to accommodate inserts designed to hold the load cells instrumentation. To measure the nip angle, a precision optical encoder (20 circuits, rotor and stator circular connectors, weather proof) was used. The rotating union and slip ring encoder were made removable from compactor for cleaning, calibration, and storage purposes.

The subminiature load cells measure the force as a function of pressure developed by compacted material in the nip area along the roll width (front, center and back) and transmitted through probes. The tip of the probe (1 mm diameter) is on the depth of 'knurling' valley and the head of the probe in contact with load cell. The probes are placed inside the bushings and the miniature wave springs are pushing the probes against the load cells to keep them in contact. The probes and bushings are installed in a removable roll segment (insert) in such a way that the probe tips and bushing faces are even when all roll components are assembled. The correct depth level for the probes tips and bushing face is controlled. The subminiature load cells are equipped with overload protection: probes come to a rigid stop when overloaded. Influence of miniature wave springs to the pressure reading is eliminated by software zero balancing.

A calibration fixture was built to enable periodic transducer calibration. Provisions were made to protect electronic components inside the roll cavities, as well as amplifiers, sensors, load cells, signal cable, rotating union, and the slip ring from powder contamination, heat and electrical failure. Side face plating over cavities was made wear resistant, brazened, and hermetically sealed so that no material could get in. All electronic components inside the roll cavities were made intrinsically safe from heat and electrical failures. Figs. 2 and 3 show the instrument roll assembly on Alexanderwerks® WP120 roller compactor.

The signals from the load cells and the encoder were sent to a stationary data acquisition system via a slip ring assembly and captured by AIM® software. In addition, AW120 roller compactor parameters (roll speed, feed screw speed, hydraulic roll pressure, and roll gap) were also acquired by AIM® software. Thus, for each run, roller compaction parameters and corresponding normal stress values were collected. Depending upon roll speed and data acquisition time, number of peaks at each run varied from 12 to 36.

2.2. Roller compaction of placebo pre-blend

A placebo blend was prepared using microcrystalline cellulose PH102 (FMC biopolymer, USA), anhydrous lactose (Kerry Bio-science, USA), croscarmellose sodium (FMC biopolymer, USA), colloidal silicon dioxide (Degussa, USA), and magnesium stearate (Mallinckrodt, USA). Placebo pre-blend composition is shown in Table 1. Intragranular portion of the placebo (i.e. pre-blend) was used for roller compaction. Pre-blend was passed through Alexanderwerk® WP120 roller compactor at various combinations of roll speed, feed screw speed, and hydraulic roll pressure as per experimental design shown in Table 2. At each roll speed, three different hydraulic roll pressures were used. At a given combination of roll speed and hydraulic roll pressure, feed screw speed values were varied to achieve various gap values within the range (i.e. 1–4 mm) recommended by equipment manufacturer. At 4 rpm roll speed, at feed screw speed equal to 19 and 25 rpm, recorded gap reached ~2.6 and 3.6 mm, respectively. Therefore, 5 rpm roll speed was included to obtain at least three different gap values at each of the three hydraulic roll pressures used. At each set of combination,

Table 1
Placebo composition.

Ingredient	% (w/w)
Intragranular	
Microcrystalline cellulose PH102	47.75
Anhydrous lactose	47.75
Magnesium stearate	0.5
Colloidal silicon dioxide	0.25
Croscarmellose sodium	1.5
Extra granular	
Magnesium stearate	0.5
Colloidal silicon dioxide	0.25
Croscarmellose sodium	1.5

Table 2
Experimental design for roller compaction of model placebo.

Roll speed (rpm)	Hydraulic roll pressure (bar)	Screw speed (rpm)
4	40	19, 25
	55	19, 25
	70	19, 25
5	40	19, 25, 31
	55	19, 25, 31
	70	19, 25, 31
8	40	25, 31, 37, 43, 49
	55	25, 31, 37, 43, 49
	70	25, 31, 37, 43, 49
12	40	31, 37, 43, 49, 53
	55	31, 37, 43, 49, 53
	70	31, 37, 43, 49, 53

Table 3
Range of drug substance and magnesium stearate levels.

	Alpha[a] (−1.4)% (w/w)	(−1) Low% (w/w)	(0) Center% (w/w)	(+1) High% (w/w)	Alpha (+1.4)% (w/w)
Drug A	3	5	10	15	17
Magnesium stearate	0.2	0.2	0.5	0.8	0.9

Drug substance properties: (d10 = 1.4 μm; d50 = 6.0 μm; d90 = 13.8 μm using LLS), internal angle of friction = 0.7751 rad, compressibility = 42.4%, bulk density = 0.36 g/cc.
[a] Alpha is a multiplier used to obtain a star point. When a star point lies outside of the cubic design, it provides a surface response design. Alpha = 1.4. At −1.4, magnesium stearate level is 0.1% (w/w). Due to sticking concerns, we used 0.2% (w/w) magnesium stearate at alpha = −1.4.

normal stress values from 3 sensors and corresponding machine parameters (i.e. roll speed, screw speed, hydraulic roll pressure, and gap) values were recorded by AIM® software. At least 3 kg of pre-blend was roller compacted at each setting.

2.3. Roller compaction of pre-blend with active A

The active pre–blends were prepared using various combinations of one active ingredient (3–17%, w/w) and lubricant (0.1–0.9%, w/w) concentrations with remaining composition made up of same ingredients as placebo pre-blend. Various active ingredient and lubricant concentrations used in this study are shown in Table 3. A factorial center composite design (2^5) was used with (1) drug concentration, (2) lubricant concentration, (3) roll speed, (4) hydraulic roll pressure, and (5) screw speed as variables as shown in Table 4. The goal of varying drug and lubricant concentration was to assess the effects of blend properties on normal stress measurements and ribbon density. As the active and lubricant concentration was changed, the % (w/w) of microcrystalline cellulose PH102 and anhydrous lactose was adjusted while maintaining their ratio at 1:1 with respect to each other. The compositions of various active blends are provided in Table 5. The blends I, J, and K shown in Table 5 are center points with respect to the composition.

At least 3 kg of pre-blend was roller compacted at each roller compactor setting. Ribbon samples were collected at each of the DOE runs for both placebo and active blends. Typically steady state was observed after approximately 1 min or 2 min confirmed by presence of steady normal stress peaks displayed by AIM® data acquisition software. After steady state, normal stress data was collected for 2–4 min depending on roll speed. Ribbon chopper on roller compactor was stopped briefly to collect intact ribbons with sufficient lengths. Intact ribbon samples provided entire ribbon width needed during ribbon density measurement for accurate measurements of average ribbon density.

After accumulation of sufficient quantity of intact ribbons, front cover was pulled to stop the machine and collect ribbon samples. Roller compactor was restarted to acquire normal stress data for additional 2–4 min and average of normal stress data (pre- and post-ribbon sample collection) was used for each set of experiment. During all the experimental work, Alexanderwerks® WP120 roller compactor was operated with vacuum de-aeration unit on.

Table 4
Study design for roller compaction of pre-blend with active drug substance A.

Blend	Batch #	Drug load (%, w/w)	Lubricant level (%, w/w)	Roll speed (rpm)	Screw speed (rpm)	SR	Roll pressure (bar)
A	1	+1	+1	12	62.4	5.2	40
	2	+1	+1	12	48	4	70
	3	+1	+1	5	26	5.2	70
	4	+1	+1	5	20	4	40
B	5	+1	−1	12	62.4	5.2	70
	6	+1	−1	12	48	4	40
	7	+1	−1	5	26	5.2	40
	8	+1	−1	5	20	4	70
C	9	−1	+1	12	62.4	5.2	70
	10	−1	+1	12	48	4	40
	11	−1	+1	5	26	5.2	40
	12	−1	+1	5	20	4	70
D	13	−1	−1	12	62.4	5.2	40
	14	−1	−1	12	48	4	70
	15	−1	−1	5	26	5.2	70
	16	−1	−1	5	20	4	40
E	17	$-\alpha$	0	8	36.8	4.6	55
F	18	$+\alpha$	0	8	36.8	4.6	55
G	19	0	$-\alpha$	8	36.8	4.6	55
H	20	0	$+\alpha$	8	36.8	4.6	55
I	21	0	0	5	23	4.6	55
	22	0	0	12	55.2	4.6	55
	23	0	0	8	32	4	55
	24	0	0	8	41.6	5.2	55
J	25	0	0	8	36.8	4.6	40
	26	0	0	8	36.8	4.6	70
	27	0	0	8	36.8	4.6	55
	28	0	0	8	36.8	4.6	55
K	29	0	0	8	36.8	4.6	55

SR: screw speed to roll speed ratio, and α (=1.4) is a multiplier for start point.

Table 5
Compositions of active blends (A to K).

Excipient	A	B	C	D	E	F	G	H	I, J,K
Intragranular									
Active	15	15	5	5	3	17	10	10	10
Magnesium stearate	0.8	0.2	0.8	0.2	0.5	0.5	0.2	0.9	0.5
Colloidal silicon dioxide	0.25	0.25	0.25	0.25	0.25	0.25	0.25	0.25	0.25
Croscarmellose sodium	1.5	1.5	1.5	1.5	1.5	1.5	1.5	1.5	1.5
MCC PH102	40.1	40.4	45.1	45.4	46.25	39.25	42.9	42.55	42.75
Anhydrous lactose	40.1	40.4	45.1	45.4	46.25	39.25	42.9	42.55	42.75
Extra granular									
Magnesium stearate	0.5	0.5	0.5	0.5	0.5	0.5	0.5	0.5	0.5
Colloidal silicon dioxide	0.25	0.25	0.25	0.25	0.25	0.25	0.25	0.25	0.25
Croscarmellose sodium	1.5	1.5	1.5	1.5	1.5	1.5	1.5	1.5	1.5

Note: All units % (w/w). Intragranular portion = 97.75% of the net batch size for all blends. Only intragranular preblends were prepared and used for roller compaction. Blends I, J, and K are center point-blend composition. Ratio of MCC PH102 to anhydrous lactose was maintained at 1:1 for all blends.

2.4. Sample testing (ribbon density measurements)

The sample mass was measured using an analytical balance (Sartorius AG, Goettingen, Germany). True densities of pre-blends were measured by AccuPyc® II 1340 Helium Gas Pycnometer (Micromeritics Instrument Co., Norcross, GA, USA). Analysis was conducted in triplicate. The pre blend samples were dried at 50 °C for 12 h prior to analysis.

The ribbon density was measured using the GeoPyc® 1360 Envelope Density Analyzer (Micromeritics Instrument Co., Norcross, GA, USA). A 25.4 mm internal diameter tube was used for the analysis. For each run, 10 replicates were used. The method used a consolidation force of 51 N and a conversion factor of 0.5153 cm^3/mm. Ribbon density measurements were done in triplicates by preparing three separate samples.

Due to feed screw geometry, normal stress across ribbon width is not uniform. For the top knurled roll and bottom knurled (instrumented) roll, the normal stress at the center of the ribbon was greater than those at both sides of the ribbon. Therefore, during the ribbon density measurements, entire ribbon width of the sample was analyzed. The sample size ranged from 3 to 4 g.

2.5. Compaction data of pre-blends

Compaction data were generated using Stylcam® compaction simulator for placebo and nine active pre-blends. Average compact weight was 400 mg. For each pre-blend, porosity and tensile strength vs. compaction pressure data were generated. A 1/4″ diameter flat faced round tooling was used with dwell time equal to approximately 100 ms.

2.6. Internal angle of friction

Internal angle of friction was measured using FT4 powder rheometer from Freeman Technologies®. Shear cell tests were performed using the FT4 powder rheometer at consolidation levels of 3, 6, 9, and 15 kPa. The powder was loaded into a 25 mm × 10 ml cylindrical split vessel and analyzed using the standard shear cell method, both provided by Freeman Technologies.

The standard test method for the shear cell test involved a conditioning step followed by a consolidation step with the vessel in the closed position, then splitting the vessel and performing a rotary shear test to create a yield locus for the prescribed consolidation level. Each shear test value of the yield locus was comprised of the maximum shear stress before incipient powder failure and pre-shear values were comprised of the average of the last 10% at steady state shear. From this data, values of internal angle of friction were automatically generated by the FT4 software using Mohr's circle analysis.

The compressibility test was initially executed as the shear cell test, where deviation occurs after the conditioning step and the vessel is split without any prior consolidation. Compressibility tests are then sequentially performed using a vented piston, provided by Freeman Technologies, at levels of 1, 2, 4, 6, 8, 10, 12, and 15 kPa. Compressibility and bulk density were derived from these results. For the above tests, sample size was less than 10 g.

2.7. Data analysis tools

JMP® 8.0 (SAS) was used for statistical analysis. The typical results presented by JMP® 8.0 (SAS) include leverage plots, least squares means, summary of Fit table, the parameter Estimates table, the effect tests table, analysis of variance, and the residual by predicted and leverage plots. In this paper we have presented leverage plot results and some of the parameter estimate tables, when appropriate.

The graphical display of an effect's significance test is called a leverage plot. Leverage plots allow graphical view of the significance of the model and provide information on whether an effect is significant. The leverage plots are shown with confidence curves. These indicate whether the test is significant at the 5% level (i.e. $p = 0.05$) by showing a confidence region for the line of fit. If the confidence region between the curves contains the horizontal line, then the effect is not significant. If the curve crosses the horizontal line, the effect is significant.

MATLAB® was used to calculate average ribbon density across ribbon width using trapezoidal rule.

3. Results and discussion

3.1. Placebo normal stress measurements

Placebo pre-blend was passed through Alexanderwerk® WP120 roller compactor at various combinations of (1) roll speed, (2) screw speed, and (3) hydraulic roll pressure as per experimental design shown in Table 2 and normal stress values of middle sensor (P2) were recorded along with machine parameters (i.e. roll speed, screw speed, hydraulic roll pressure, and gap). The measured values of roll speed, feed screw speed, hydraulic roll pressure and the corresponding gap, normal stress and ribbon density values are presented in Table 6. For the top knurled roll and bottom instrumented knurled roll, it was noted that normal stress values recorded by middle sensor (P2), were uniform for a given settings of roll speed, feed screw speed, and hydraulic roll pressure. Normal stress values recorded by side sensors (P1) and (P3) were lower than normal stress values recorded by middle sensor (P2) and showed greater variability than middle sensor (P2). This is attributed to heterogeneity of feeding pressure in the last flight of the feed screw and this has

Table 6
Average placebo ribbon densities (profiles 1 and 2) calculated using normal stress data P1, P2, and P3.

Actual feed screw (rpm)	Actual roll pressure (bar)	Actual roll speed (rpm)	Gap (mm)	P1 (MPa)	P2 (MPa)	P3 (MPa)	Profile 1 average density (g/cc)	Exp average density GeoPyc (g/cc)	Profile 2 average density (g/cc)
18.70	42.10	3.98	2.65	37.50	68.90	35.15	1.0034	1.0426	1.0228
24.70	41.50	3.97	3.63	32.10	55.40	23.70	0.9515	1.0093	0.9700
18.70	57.15	3.97	2.51	46.30	94.40	51.50	1.0748	1.1148	1.0967
24.60	56.35	3.96	3.43	37.70	77.30	30.10	1.0007	1.0827	1.0258
18.70	73.00	3.96	2.40	52.35	122.55	70.60	1.1337	1.1737	1.1569
24.60	72.30	3.93	3.27	42.55	103.55	49.35	1.0698	1.1378	1.0966
18.70	41.10	4.98	2.05	39.00	73.90	44.90	1.0312	1.0720	1.0491
24.70	42.15	4.97	2.82	35.80	66.05	34.50	0.9956	1.0385	1.0144
30.50	41.90	4.96	3.59	33.10	57.50	28.05	0.9663	1.0323	0.9839
18.70	56.90	4.96	1.94	52.80	104.25	65.35	1.1165	1.1317	1.1359
24.70	57.65	4.95	2.65	45.80	91.10	50.10	1.0689	1.1159	1.0902
30.50	56.55	4.94	3.38	43.10	78.35	40.60	1.0349	1.0872	1.0550
18.70	72.80	4.95	1.87	63.30	132.55	85.15	1.1759	1.1589	1.1951
24.70	73.50	4.94	2.55	60.10	119.40	66.75	1.1397	1.1596	1.1609
30.50	71.90	4.93	3.24	48.30	101.65	52.15	1.0847	1.1465	1.1083
18.70	41.20	7.97	1.16	52.00	81.30	62.80	1.0942	1.0716	1.1061
24.70	41.10	7.97	1.64	50.30	74.83	50.83	1.0651	1.0546	1.0780
30.60	41.35	7.97	2.12	41.00	71.40	44.45	1.0320	1.0296	1.0483
36.60	41.60	7.97	2.60	39.25	67.95	37.95	1.0120	1.0296	1.0293
42.60	42.15	7.96	3.07	36.10	62.75	33.80	0.9913	1.0144	1.0085
24.70	56.55	7.97	1.54	62.85	108.05	74.90	1.1497	1.1393	1.1651
30.60	57.60	7.96	1.98	54.60	102.75	65.45	1.1189	1.0818	1.1372
36.60	57.90	7.96	2.42	50.30	96.05	55.30	1.0901	1.0867	1.1103
42.60	57.05	7.95	2.87	46.55	88.65	48.90	1.0662	1.0772	1.0867
48.50	55.70	7.95	3.33	44.00	80.45	37.50	1.0322	1.0635	1.0539
24.70	71.50	7.97	1.46	71.20	138.10	96.35	1.2027	1.1931	1.2188
30.60	71.80	7.96	1.87	64.07	131.20	84.37	1.1756	1.1394	1.1945
36.60	73.15	7.95	2.30	61.50	124.60	74.45	1.1556	1.1414	1.1759
42.50	73.10	7.94	2.73	53.75	115.50	65.80	1.1254	1.1439	1.1477
48.50	72.35	7.93	3.17	53.80	105.05	55.90	1.1034	1.1203	1.1253
36.60	57.13	7.95	2.43	45.83	94.50	54.30	1.0789	1.1119	1.1002
36.60	57.30	7.95	2.44	47.65	95.10	54.95	1.0839	1.0948	1.1047
24.70	40.50	12.00	0.99	46.85	78.25	71.25	1.0949	1.0567	1.1049
30.60	40.50	12.00	1.27	47.60	77.80	61.00	1.0802	1.0461	1.0924
36.70	40.65	12.00	1.59	44.50	76.80	53.45	1.0606	1.0667	1.0754
42.60	40.95	12.00	1.89	41.60	73.45	47.55	1.0411	1.0617	1.0571
48.65	41.40	12.00	2.20	38.65	70.80	42.95	1.0237	1.0174	1.0410
54.70	41.15	12.00	2.52	36.90	66.85	37.45	1.0050	1.0213	1.0228
30.60	55.80	12.00	1.20	64.00	110.30	84.40	1.1652	1.1376	1.1789
36.70	55.75	12.00	1.49	59.45	106.85	74.90	1.1435	1.1440	1.1594
42.60	56.00	12.00	1.78	54.60	105.15	67.55	1.1236	1.0750	1.1422
48.60	56.80	12.00	2.08	52.10	99.85	61.70	1.1067	1.1258	1.1258
54.70	56.75	12.00	2.38	48.55	94.50	55.70	1.0865	1.0901	1.1065
30.60	72.55	12.00	1.16	74.30	139.35	105.75	1.2168	1.2130	1.2309
36.70	72.35	12.00	1.44	72.70	139.65	98.25	1.2074	1.1792	1.2231
42.60	70.50	12.00	1.71	65.60	130.10	87.75	1.1816	1.1676	1.1991
48.60	72.90	12.00	1.98	64.15	131.90	81.40	1.1723	1.1470	1.1919
54.60	71.95	12.00	2.27	60.40	122.95	71.75	1.1493	1.1514	1.1701

also been previously reported in the literature (Simon and Guigon, 2003). The tip of the Alexanderwerks® feed screw is approximately 10 mm and is consistently delivering uniform flow of the powder blend into the nip zone and hence it is applying steady feed pressure resulting in steady normal stress (P2) at the center of the roll. Therefore, normal stress values (P2) recorded at various combinations of roll speed, feed screw speed, and hydraulic roll pressure were used for data analysis.

The normal stress values (P2) were used as output response. The roll speed (R), screw speed to roll speed ratio (SR), and hydraulic roll pressure (HP) were used as input factors. The dimensionless factor SR influences the gap between the rolls. The Standard Least Squares fitting was used with continuous-response (P2) fit to a linear model of factors (R, SR, and HP) using JMP® 8.0 (SAS) as described in Section 2.7.

Roll speed and its interaction with remaining factors were found to be not significant and not included in final model. Final linear model included only significant factors and their interactions. The model fit summary and parameter estimates are provided in Tables 7 and 8, respectively. The normal stress (P2) is related to hydraulic roll pressure (HP) and screw speed to roll speed ratio (SR) as follows:

$$P2 = 31.233631 + 1.8283263 \times (HP) - 8.829931 \times (SR) - 0.15084 \times (HP - 56.4975) \times (SR - 4.32091) \quad (1)$$

Fig. 4 shows leverage plots of normal stress (P2) vs. screw speed to roll speed ratio (SR), and hydraulic roll pressure (HP). As can be seen from the data, hydraulic roll pressure (HP), and screw to roll speed ratio (SR) had significant effect on normal stress (P2).

Table 7
Summary of fit for normal stress (P2) vs. hydraulic roll pressure (HP) and screw speed to roll speed ratio (SR) for placebo blend.

R^2	0.99608
R^2 adjusted	0.995813
Root mean square error	1.55153
Mean of response	96.03396
Observations (or sum Wgts)	48

Table 8
Parameter estimates for normal stress (P2) vs. hydraulic roll pressure (HP) and screw speed to roll speed ratio (SR) for placebo blend.

Term	Estimate	Standard error	*t* ratio	Prob > |*t*|
Intercept	31.233631	1.254968	24.89	<.0001
HP	1.8283263	0.018192	100.50	<.0001
SR	−8.829931	0.196475	−44.94	<.0001
(HP − 56.4975) × (SR − 4.32091)	−0.15084	0.015164	−9.95	<.0001

Normal stress (P2) increased as hydraulic roll pressure (HP) increased, with factor (SR) fixed at center point of the data set. Normal stress (P2) decreased as feed screw speed to roll speed ratio (SR) increased, with factor (HP) fixed at center point of data set. As screw speed to roll speed ratio (SR) increased at a given hydraulic roll pressure, more material is passed through the rolls and upper roll is pushed upward, thus resulting in a decrease in normal stress (P2). Roll speed effect on P2 was absent for the placebo blend evaluated in this study. These findings are consistent with those reported by Meyer et al. (2005). Johanson (1965) reported that the logarithmic ratio of peak pressure feed pressure (i.e. $\log(\sigma_m/\sigma_0)$) decreased as the dimensionless ratio of gap to roll diameter (S/D) increased. The ratio of peak pressure to feed pressure and dimensionless ratio of gap to roll diameter reported by Johanson (1965) are analogous to P2 and SR reported in this study, respectively.

Using gravity-fed system; Bindhumadhavan et al. (2005) have reported that the peak normal pressure decreased as the roll speed increased. They assumed that this phenomenon was due to increased entrapment of air. However, information about gravity feed rates or ribbon density data was not reported in their work. We suggest that, as the roll speed increased, more material was pulled in by the counter-rotating rolls causing increase in SR (feed to roll speed ratio) and subsequently causing decrease in peak normal pressure according to Eq. (1).

The placebo pre-blend consisted of 1:1 ratio of microcrystalline cellulose PH102 (viscoelastic) and anhydrous lactose (brittle), and therefore strain rate effect was expected to be minimal. For blends predominantly consisting of viscoelastic (e.g. microcrystalline cellulose PH102) or plastic (e.g. pregelatinized starch) excipients, roll speed effect could be present and need to be verified experimentally.

3.2. Placebo ribbon density model

Ribbon density of placebo runs were analyzed as a function of normal stress (P2) and gap. Fig. 5 shows leverage plots for ribbon density as a function of normal stress (P2) and measured gap (*G*). Ribbon density was mainly function of normal stress (P2). Within the gap range recorded, ribbon density was independent of gap (*G*) (i.e. $p = 0.1529$).

Thus, final general linear model relating placebo ribbon density to the normal stress (P2) is given by Eq. (2).

$$\text{Ribbon density} = 0.9014067 + 0.0020673(\text{P2}) \quad (2)$$

Thus, ribbon density increased as the normal stress (P2) increased. These findings are consistent with those reported by Meyer et al. (2005). Thus, if one were to increase the material throughput on a given roller compactor by increasing screw speed to roll speed ratio and keep same ribbon density, it will be necessary to increase hydraulic roll pressure to maintain same normal stress as before to achieve same ribbon density. Eq. (1) can be used to estimate new value of hydraulic roll pressure (HP) for a new value of screw speed to roll speed ratio (SR) to maintain same normal stress P2 on the ribbon. By maintaining the same normal stress (P2) on ribbon as before, one would obtain same ribbon density as predicted by Eq. (2).

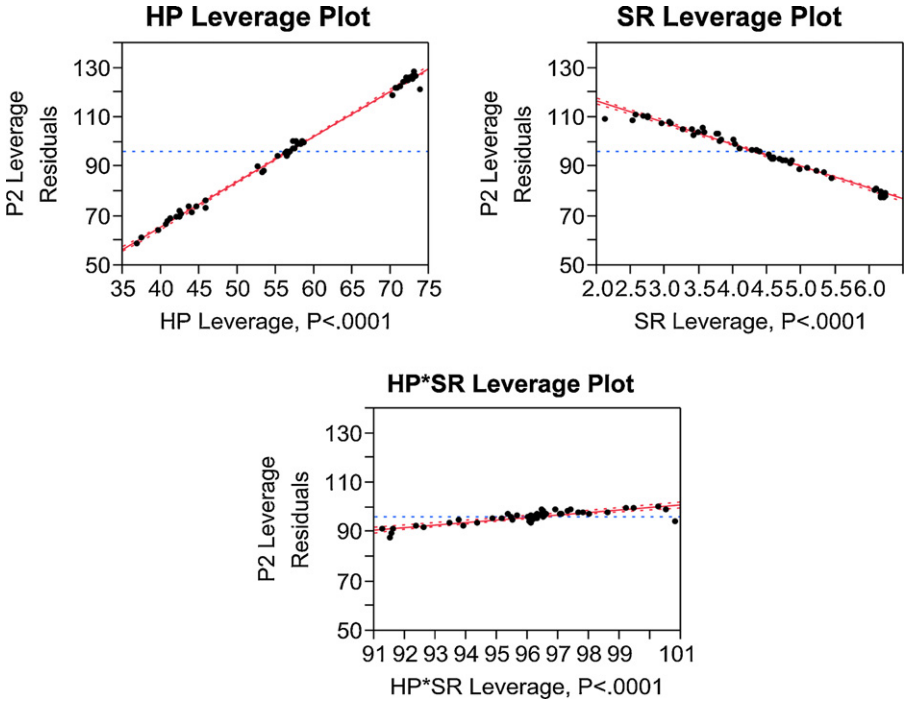

Fig. 4. Leverage plots of normal stress (P2) vs. screw speed to roll speed ratio (SR), and hydraulic roll pressure (HP) for placebo formulation.

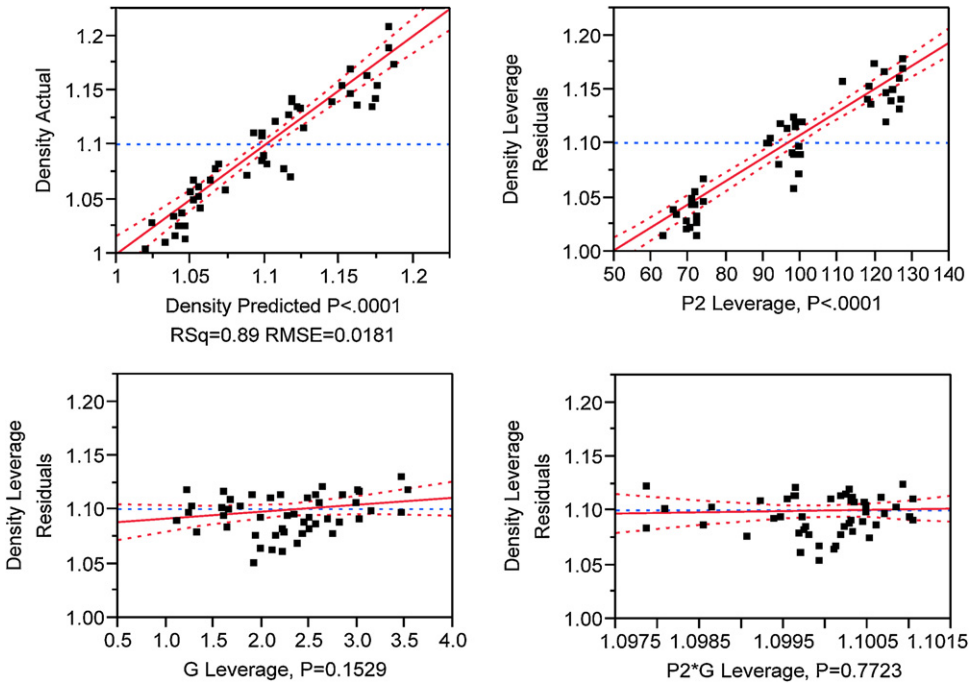

Fig. 5. Leverage plots of placebo ribbon density as a function of normal stress (P2) and roll gap (*G*).

3.3. *Placebo ribbon density prediction using porosity–pressure data of pre-blend*

Porosity vs. compaction pressure data of placebo blend (Table 9) generated using Stylcam compaction simulator was used to estimate average ribbon density. The true density of placebo blend was measured to be 1.5587 g/cc. As mentioned in Section 3.1, the tip of the Alexanderwerks® feed screw is approximately 10 mm and deliver uniform flow of the powder blend into the nip zone. Therefore, feed screw applies steady feed pressure resulting in steady normal stress (P2) at the center of the ribbon. The normal stress values recorded by side sensors (P1 and P3) are smaller than P2 for the top knurled and bottom knurled roll combination.

For the estimation of average ribbon density, two normal stress profiles were evaluated as shown in Figs. 6 and 7. Using true density of pre-blend and compaction data (i.e. out of die porosity vs. compaction pressure), and normal ribbon stress data (P1, P2, and P3), ribbon density across the ribbon width is calculated for each placebo run using both profiles. The average ribbon density across ribbon width is calculated by trapezoidal rule using MATLAB®. The normal ribbon stress data (P1, P2, and P3) for placebo runs and corresponding average ribbon densities calculated using profiles 1 and 2 are provided in Table 6.

The calculated average ribbon densities were compared with experimentally measured ribbon densities using GeoPyc®. Root mean square errors (RMSE) were calculated using calculated vs. experimental ribbon densities. The following Eq. (3) was used to estimate RMSE.

$$\text{RMSE} = \sqrt{\frac{\sum_1^N (\rho_{celc} - \rho_{\text{exp}})^2}{N}} \quad (3)$$

N is number of observations in data set, ρ_{calc} is calculated ribbon density and ρ_{exp} is experimentally ribbon density.

To calculate %RSD, mean value of experimental data set is used. RMSE for profile 1 was equal to 0.033232 (%RSD = 3.02) and RMSE for profile 2 was equal to 0.030498 (%RSD = 2.77). Therefore, for the remaining data analysis, profile 2 was used. As can be seen from Figs. 8 and 9, estimated average ribbon densities of placebo batches prepared at various combination of roller compactor parameters

Table 9
Compaction data of placebo pre-blend.

Mean compression force (MPa)	Out of die porosity	Tensile strength (Mpa)
27.7	41.9	0.180
35.3	38.3	0.302
45.8	34.4	0.482
62.3	29.8	0.859
83.5	24.4	1.447
113.7	19.7	2.271
154.3	15.9	3.266
209.5	11.9	4.602
277.0	9.5	5.554

True density of placebo pre blend = 1.5587 g/cc.

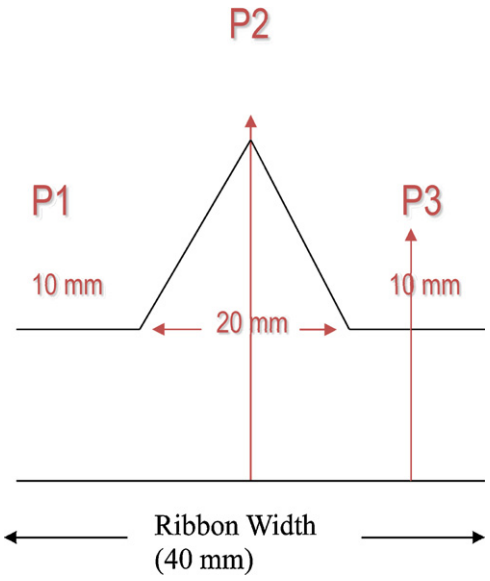

Fig. 6. Normal stress profile 1.

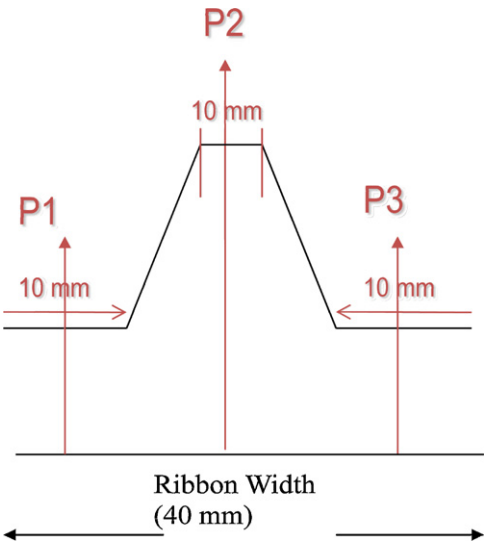

Fig. 7. Normal stress profile 2.

compared well with experimentally measured average ribbon densities by GeoPyc instrument. Thus, density–pressure equations for a given pre-blend can be included in AIM software to display on line ribbon density data during roller compaction runs.

3.4. Active blend normal stress measurements

Active pre-blends were passed through Alexanderwerk® WP120 roller compactor at various combinations of (1) roll speed, (2) screw speed, and (3) hydraulic roll pressure as per experimental design shown in Table 4 and normal stress values of middle sensor (P2) were recorded along with machine parameters (i.e. roll speed, screw speed, hydraulic roll pressure, and gap). The normal stress values (P2) was used as output response. The roll speed (R), screw speed to roll speed ratio (SR), and hydraulic roll pressure (HP), and compressibility (K) were used as input factors. Compressibility (K) is defined as the inverse of slope of ascending linear region

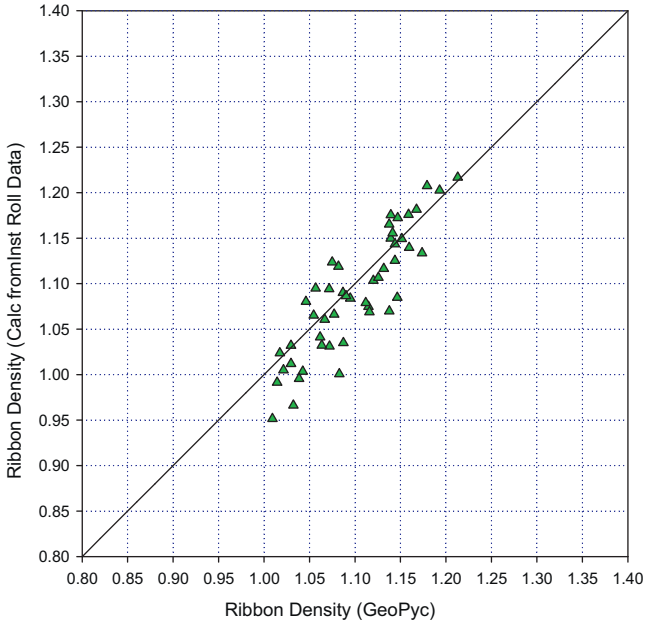

Fig. 8. Average ribbon density of placebo runs. Comparison of experimentally measured (GeoPyc) vs. calculated using normal stress data and normal stress profile 1. RMSE = 0.033232 (%RSD = 3.02).

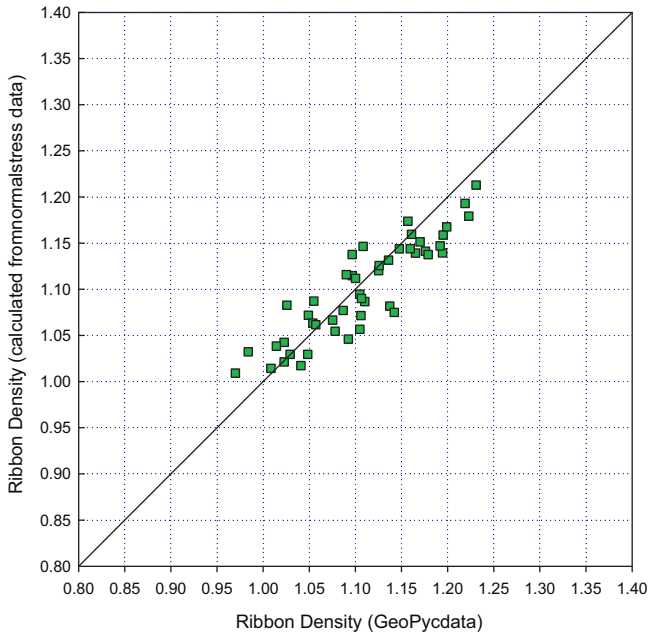

Fig. 9. Average ribbon density of placebo runs. Comparison of experimentally measured (GeoPyc) vs. calculated using normal stress data and normal stress profile 2. RMSE = 0.030498 (%RSD = 2.77).

of log(D) vs. log(P) curve where D is compact density and P is normal stress measured for pre-blends using Stylcam® compaction simulator. The calculation procedure for compressibility (K) is described in work done by Bindhumadhavan et al. (2005). The dimensionless factor SR influences the gap between the rolls.

Normal stress (P2) was analyzed as a function of hydraulic roll pressure (HP), feed screw speed to roll speed ratio (SR), compressibility (K) using JMP® 8.0 (SAS) as described in Section 2.7. In this paper we have presented mainly leverage plot results and some of the parameter estimate tables, when appropriate. Tables 10 and 11 show model fit output and parameter estimates.

Roll speed and its interaction with remaining factors were found to be not significant and not included in final model. Final linear model included only significant factors and their interactions, when present. The normal stress (P2) is related to hydraulic roll pressure (HP) and screw speed to roll speed ratio (SR), compressibility (K) as follows:

$$P2 = 38.658621 + 1.7168196 \times (\mathrm{HP}) - 12.03276 \times (\mathrm{SR}) - 0.197369 \times (\mathrm{HP} - 56.9793) \times (\mathrm{SR} - 4.57034) + 3.0260294 \times K \quad (4)$$

As can be seen from Fig. 10, although compressibility (K) was found to be significant, the rate of change of P2 vs. K was lower than that of P2 vs. hydraulic roll pressure (HP).

Similar to placebo pre-blend, for active pre-blends, the normal stress (P2) increased as hydraulic roll pressure (HP) increased, with remaining factors fixed at their corresponding center points. Normal stress (P2) decreased as screw speed to roll speed ratio

Table 10
Summary of fit for normal stress (P2) vs. hydraulic roll pressure (HP) and feed screw speed to roll speed ratio (SR), and compressibility (K) for active blend.

R^2	0.99246
R^2 adjusted	0.991203
Root mean square error	2.122212
Mean of response	96.99655
Observations (or sum Wgts)	29

Table 11
Parameter estimates for normal stress (P2) vs. hydraulic roll pressure (HP) and feed screw speed to roll speed ratio (SR), and compressibility (*K*) for active blend.

Term	Estimate	Standard error	*t* ratio	Prob > |*t*|
Intercept	38.658621	6.210537	6.22	<.0001
HP	1.7168196	0.031894	53.83	<.0001
(HP − 56.9793) × (SR − 4.57034)	−0.197369	0.056285	-3.51	0.0018
SR	−12.03275	0.826972	-14.55	<.0001
K	3.0260294	0.876239	3.45	0.0021

(SR) increased. As screw speed to roll speed ratio (SR) increased at a given hydraulic roll pressure, more material is passed through the rolls and upper roll is pushed upward, thus resulting in a decrease in normal stress P2.

3.5. Active ribbon density model

Ribbon densities of active blends were analyzed as a function of normal stress (P2) and gap. Ribbon density of active batches was related to normal stress and gap by following Eq. (5).

$$\text{Ribbon density} = 0.8440952 + 0.0021527(\text{P2}) + 0.0276773(\text{Gap}) \quad (5)$$

Table 12 shows comparison of statistical general linear model predicted (Eq. (5)) and experimentally measured (i.e. GeoPyc®) ribbon densities of active batches. Root mean square error (RMSE) was calculated to be 0.01624 (i.e. 1.44%RSD) using Eq. (3).

3.6. Active ribbon density prediction using porosity–pressure data

Porosity vs. compaction pressure data of active blends (Tables 13 and 14) generated using Stylcam® compaction simulator was used to estimate average ribbon density of active batches.

For the estimation of average ribbon density, normal stress profile 2 as shown in Fig. 7 was used. Using true density, compaction (i.e. out of die porosity vs. compaction pressure), and normal stress data (P1, P2, and P3) of active pre-blends, the ribbon density across the ribbon width is calculated for each active run. The average ribbon density across ribbon width is calculated by trapezoidal rule using MATLAB®. As can be seen from Fig. 11, estimated average ribbon densities of active batches prepared at various combination of roller compactor parameters compared well with experimentally measured average ribbon densities by GeoPyc® instrument.

This work also illustrates the feasibility of on-line prediction of average ribbon density using pre-blend compaction data (i.e. solid fraction vs. normal pressure) and normal stress data on ribbon collected by the instrumented roll. Density–pressure equations for a given pre-blend can be included in AIM® software to display on line ribbon density data during roller compaction runs. This approach can be used as another Process Analytical Tool technique in addition to on-line NIR ribbon density measurements reported by Gupta et al. (2005). On-line NIR measurements can be challenging due to dusty environment at the ribbon exit and ribbon curvature/splitting issues. If both the rolls are knurled, in general ribbons tend to split, depending on combination of roller compaction parameter setting. In addition, both on development and commercial roller compactors, a flake crusher is used to break ribbon into smaller pieces before an entry into milling chamber. The instrumented roll technique with on-line ribbon density calculations can allow proper process control to maintain suitable ribbon density.

3.7. Active ribbon density prediction using placebo model

In this section, statistical models developed for placebo formulation were used to predict ribbon densities of active batches.

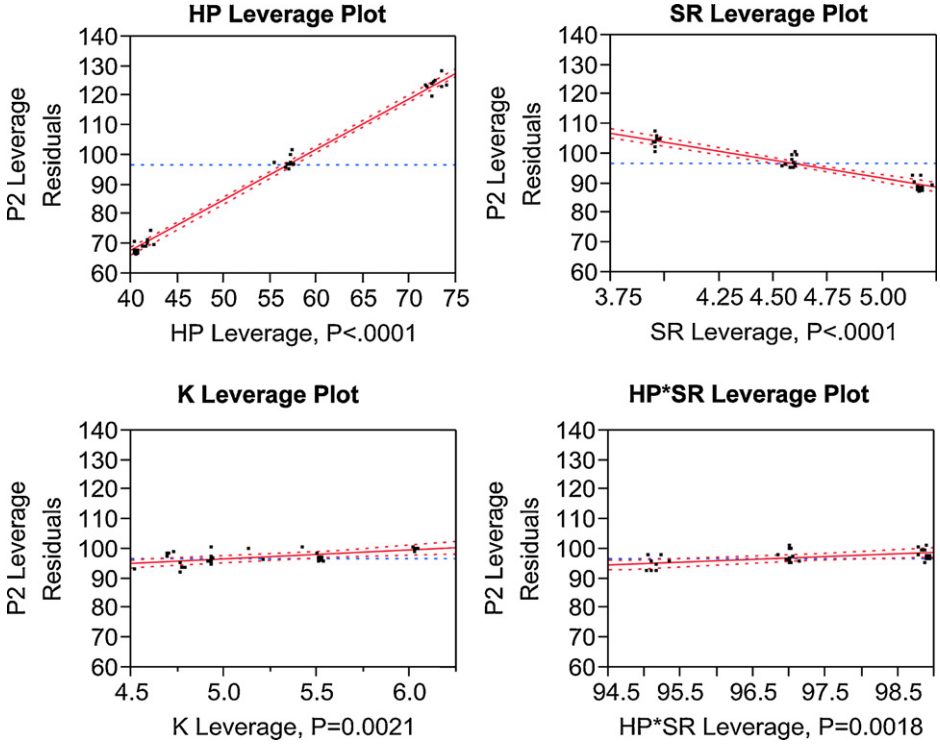

Fig. 10. leverage plots of normal stress (P2) vs., feed screw speed to roll speed ratio (SR), hydraulic roll pressure (HP), and compressibility (*K*) for active formulation.

Table 12
Comparison of predicted vs. experimentally measured ribbon densities of active batches using active ribbon density model.

Blend	Batch	Drug load (%, w/w)	P2 (Mpa)	Gap (mm)	Compressibility (*K*)	Internal angle of friction (rad)	Predicted ribbon density (g/cc)	Exp ribbon density (g/cc)
A	1	15	66.15	3.42	5.51	0.7263	1.0810	1.0787
	2	15	135.90	2.38	5.51	0.7263	1.2025	1.2126
	3	15	114.20	3.26	5.51	0.7263	1.1802	1.2002
	4	15	74.45	2.66	5.51	0.7263	1.0780	1.1124
B	5	15	116.00	2.89	6.02	0.7388	1.1738	1.1713
	6	15	77.50	2.42	6.02	0.7388	1.0778	1.0962
	7	15	67.70	3.28	6.02	0.7388	1.0805	1.1111
	8	15	137.80	2.31	6.02	0.7388	1.2045	1.2067
C	9	5	111.30	2.86	4.77	0.6454	1.1628	1.1596
	10	5	72.95	2.36	4.77	0.6454	1.0663	1.0659
	11	5	61.80	3.24	4.77	0.6454	1.0667	1.0494
	12	5	129.45	2.20	4.77	0.6454	1.1835	1.1836
D	13	5	66.15	2.97	4.70	0.6460	1.0686	1.0363
	14	5	133.10	2.05	4.70	0.6460	1.1872	1.1810
	15	5	116.20	2.80	4.70	0.6460	1.1717	1.1466
	16	5	77.05	2.31	4.70	0.6460	1.0739	1.0636
E	17	3	93.25	2.58	4.52	0.6350	1.1162	1.0831
F	18	17	96.95	2.99	5.13	0.6989	1.1356	1.1296
G	19	10	100.60	2.67	5.41	0.6809	1.1346	1.1412
H	20	10	96.55	2.76	5.21	0.6978	1.1282	1.1371
I	21	10	96.55	2.77	4.93	0.6861	1.1285	1.1364
	22	10	95.20	2.69	4.93	0.6861	1.1233	1.1354
	23	10	102.65	2.35	4.93	0.6861	1.1300	1.1511
	24	10	88.30	3.16	4.93	0.6861	1.1216	1.1277
J	25	10	68.25	2.90	4.93	0.6931	1.0713	1.0673
	26	10	123.95	2.66	4.93	0.6931	1.1845	1.1791
	27	10	96.50	2.76	4.93	0.6931	1.1281	1.1097
	28	10	95.85	2.75	4.93	0.6931	1.1264	1.1305
K	29	10	100.60	2.72	4.93	0.6966	1.1359	1.1218

The objective of this analysis was to establish upper limit of API concentrations for which placebo models can be used. Placebo normal stress model (Eq. (1)) was used to predict normal stress P2 at roller compactor settings used to prepare active batches (Table 4).

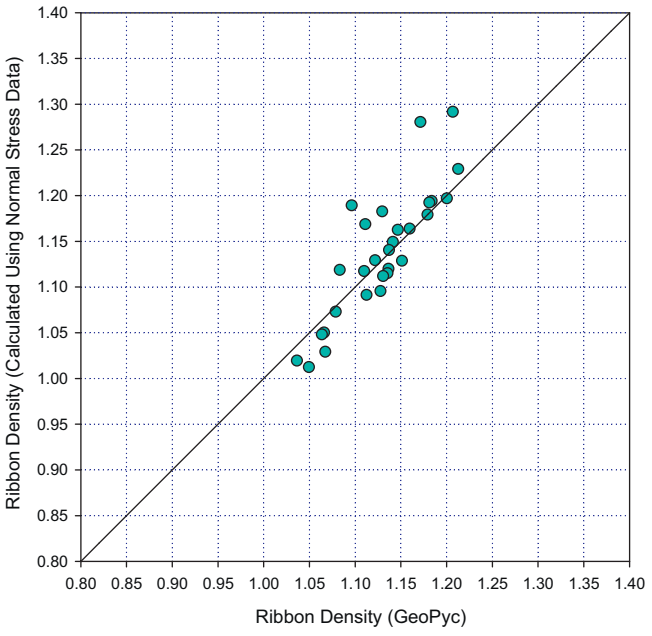

Fig. 11. Comparison of active blend ribbon density calculated using normal stress across ribbon width and compaction data vs. average ribbon density measured using GeoPyc.

Using P2 values predicted by placebo model, ribbon density of active batches were calculated using placebo ribbon density model (Eq. (2)). Experimentally measured (GeoPyc) and model predicted ribbon densities of active batches using placebo formulation are shown in Table 15.

Root mean square errors were calculated using placebo model predicted vs. experimental ribbon densities. The following Eq. (6) was used to estimate RMSE.

$$\mathrm{RMSE} = \sqrt{\frac{\sum_1^N (\rho_{\mathrm{model}} - \rho_{\mathrm{exp}})^2}{N}} \quad (6)$$

N is number of observations in data set, ρ_{model} is model predicted ribbon density and ρ_{exp} is experimentally ribbon density.

Prediction error analysis was done by selecting active runs with drug concentration ranges. For example, set 1 consisted of 3–17% (w/w) drug load blends, set 2 consisted of 3–10% (w/w) drug load blends, and set 3 consisted of 3–5% drug load blends. Table 16 shows root mean square errors and corresponding %RSDs were calculated using placebo model predicted vs. experimental active ribbon densities for each of the above mentioned sets.

Using active ribbon density data shown in Table 12, the RMSE and %RSD for the active ribbon density model were calculated to be 0.01624 and 1.44%, respectively. The RMSE for the placebo model predicted vs. experimentally measured placebo ribbon density was equal to 0.0181 (JMP output shown in Fig. 5).

The %RSD as a function of drug load concentration is shown in Fig. 12. The %RSD of the prediction increased as the % drug load of active formulations increased. However, even up to 17% (w/w) active concentration, the placebo model was able to predict ribbon density with reasonable error ($\leq$ 5%).

Table 13
Compaction data of active pre-blends (A through E).

Active blend	True density (g/cc)	Mean compression force (Mpa)	Out of die porosity	Tensile strength (Mpa)
A	1.5036	25.4	36.7	0.094
		38.2	31.4	0.213
		52.1	26.9	0.449
		74.9	22.0	0.879
		101.8	17.8	1.416
		146.3	13.2	2.399
		159.6	12.1	2.675
		233.9	8.8	3.842
B	1.5082	18.9	36.8	0.133
		25.7	30.8	0.288
		36.1	27.1	0.525
		49.6	20.9	1.017
		84.6	16.6	1.860
		134.6	11.5	2.913
		203.3	7.9	4.586
C	1.5306	21.6	42.9	0.057
		25.9	40.7	0.085
		34.9	36.8	0.157
		47.1	32.1	0.339
		66.1	28.0	0.581
		93.8	21.4	1.171
		132.5	17.0	1.825
		180.2	13.0	2.631
		244.9	9.5	3.447
D	1.5365	22.1	43.7	0.082
		31.9	39.0	0.185
		41.8	34.9	0.323
		57.2	30.1	0.603
		78.9	25.7	0.952
		108.2	20.5	1.635
		146.1	16.1	2.442
		192.7	12.6	3.448
		262.0	10.0	4.545
E	1.5346	19.3	44.9	0.063
		26.4	40.8	0.127
		35.2	36.7	0.226
		46.1	32.7	0.402
		62.6	27.8	0.716
		84.6	23.4	1.206
		117.1	17.9	1.943
		162.9	13.6	2.985
		226.1	9.7	4.191

Table 16 also shows average values of compressibility and internal angle of friction. The average value of compressibility and internal angle of friction for each set was calculated using corresponding data points from each set. For example, average value of compressibility and internal angle of friction for set 3 was calculated using all active blends with 3–5% (w/w) active concentrations (i.e. blends C, D, and E in Table 12).

As can be seen from Figs. 13 and 14, %RSD decreased as averaged values of effective angle of friction and compressibility (K) of active pre-blends approached those of placebo pre-blend.

Thus, data seem to indicate that effective angle of friction and compressibility (K) properties of active pre blend can be used as key indicators for predicting ribbon densities of active blend using placebo ribbon density model. Additional work using pre-blends with various combinations of internal angle of friction and compressibility values will be useful to further support these findings.

The Carr's index is an overall manifestation of particle size distribution. Use of Carr's index for predicting dissolution rates of acetaminophen has been reported by Lee and Hsu (2007). Their research showed that the dissolution rate constant of acetaminophen was linearly related to Carr's index of formulated dry blends prepared using API with different particle size.

Using similar approach, as an extension of this study, one could evaluate the effects of Carr's index of pre-blends prepared using API lots with different particle size on the normal stress measurements. This information could be useful in setting API particle size distribution specifications.

It has been reported by Herting and Kleinebudde (2007) that using smaller MCC particles during roller compaction led to larger granules and reduced fines. The particle size distribution of excipients can influence the ribbon properties and therefore granulation properties. The roller compaction behavior of different types of lactose was evaluated by Inghelbrecht and Remon (1998). Their studies showed that the hydraulic roll pressure, roll speed, vertical and horizontal screw speeds were found to be important during compaction of the lactose types investigated. Hydraulic roll pressure was the most important parameter. A high hydraulic roll pressure and a low horizontal screw speed at high roll speed resulted in the best granule quality. An influence of particle size and particle morphology was also demonstrated by these researchers.

Thus, it is important to evaluate multiple lots of critical excipients such as MCC, lactose, magnesium stearate during development work. The Carr's Index approach may also be extended to study effects of particles size distribution of excipients on normal stress measurements. The normal stress measurements on ribbon as a function of bulk property of an excipient (e.g. Carr's index) may help establish particle size distribution specification used in the formulation. These studies can be part of the future work.

Table 14
Compaction data of active pre-blends (F through I).

Active blend	True density (g/cc)	Mean compression force (MPa)	Out of die porosity (%)	Tensile strength (MPa)
F	1.5018	14.3	41.5	0.037
		20.2	38.5	0.077
		33.3	33.2	0.195
		46.5	28.1	0.415
		56.7	21.4	0.963
		81.3	18.5	1.517
		122.3	13.0	2.729
		173.0	9.5	3.894
		245.7	7.3	4.810
G	1.5222	19.0	41.8	0.073
		26.4	38.2	0.128
		36.1	33.6	0.256
		50.2	29.9	0.476
		73.9	24.0	0.966
		113.7	18.3	1.995
		158.6	14.4	2.971
		199.1	10.9	4.292
		266.6	8.1	5.609
H	1.5169	16.7	43.5	0.046
		24.9	37.7	0.111
		34.8	33.8	0.210
		48.7	30.5	0.390
		69.3	24.6	0.767
		98.4	19.3	1.386
		137.9	14.9	2.305
		189.1	11.6	3.253
		255.4	8.2	4.399
I, J, and K	1.5232	15.2	46.2	0.028
		17.8	43.9	0.041
		23.9	40.7	0.074
		45.3	32.8	0.291
		65.5	27.3	0.610
		95.9	21.3	1.262
		133.1	16.1	2.047
		187.3	12.0	3.120
		258.7	10.5	4.296

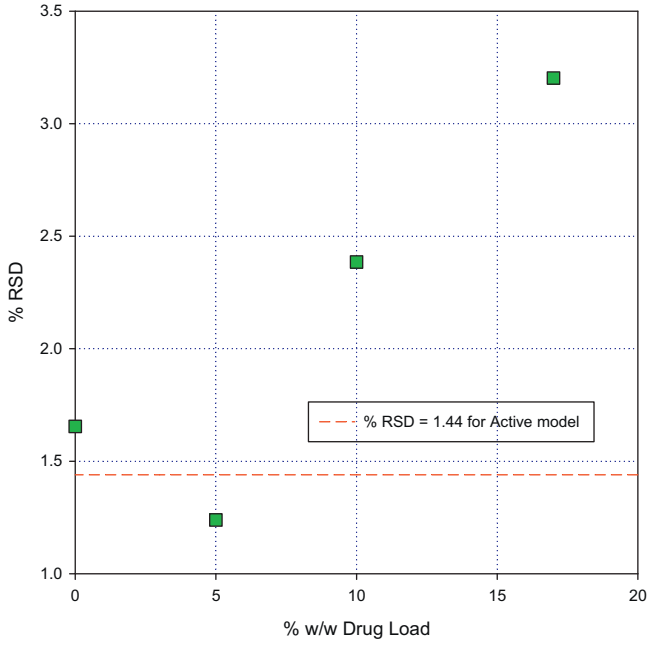

Fig. 12. %RSD of active blends ribbon density prediction using placebo model as a function of drug load.

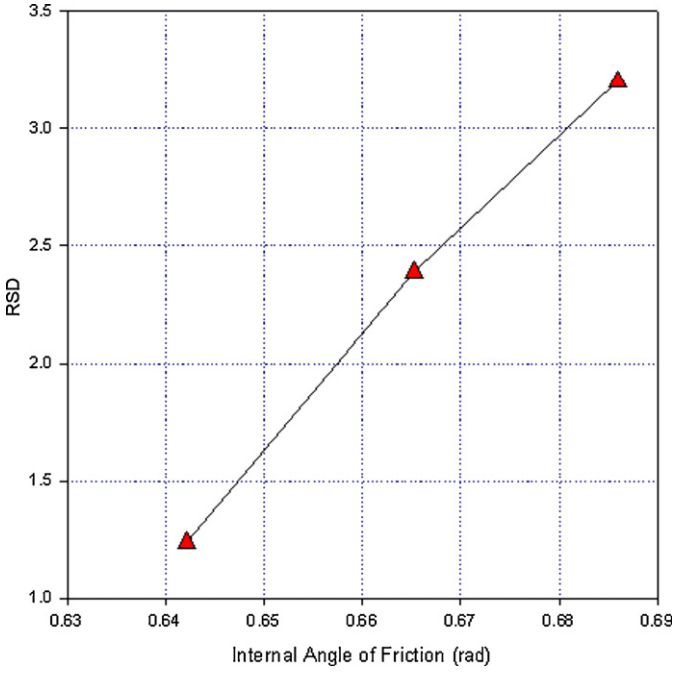

Fig. 13. %RSD as a function of internal angle of friction for the active blends ribbon density predictions using placebo model. (Internal angle of friction for placebo = 0.618 rad.)

Table 15
Comparison of placebo model predicted vs. experimentally measured ribbon densities of active batches.

Batch	Drug load (%, w/w)	Gap (mm)	Feed screw speed (rpm)	Hydraulic roll pressure (bar)	SR (feed screw to roll speed ratio)	Predicted normal stress P2 (Mpa)	Predicted ribbon density (g/cc)	Exp ribbon density (g/cc)
1	15	3.42	62.00	41.45	5.167	63.32	1.0323	1.0787
2	15	2.38	47.40	73.15	3.950	131.03	1.1723	1.2126
3	15	3.26	25.50	73.00	5.162	117.03	1.1433	1.2002
4	15	2.66	19.60	41.35	3.944	71.15	1.0485	1.1124
5	15	2.89	61.60	71.05	5.133	114.03	1.1371	1.1713
6	15	2.42	47.50	40.65	3.958	69.74	1.0456	1.0962
7	15	3.28	25.50	41.85	5.141	64.17	1.0341	1.1111
8	15	2.31	19.60	73.25	3.960	131.11	1.1724	1.2067
9	5	2.86	62.00	72.60	5.167	116.29	1.1418	1.1596
10	5	2.36	47.50	40.85	3.958	70.11	1.0464	1.0659
11	5	3.24	25.60	41.40	5.161	63.27	1.0322	1.0494
12	5	2.20	19.60	73.25	3.960	131.11	1.1724	1.1836
13	5	2.97	61.70	41.30	5.142	63.22	1.0321	1.0363
14	5	2.05	47.60	72.55	3.967	129.71	1.1696	1.1810
15	5	2.80	25.60	72.55	5.182	116.03	1.1413	1.1466
16	5	2.31	19.70	41.30	3.964	70.92	1.0480	1.0636
17	3	2.58	36.60	57.15	4.598	95.10	1.0980	1.0831
18	17	2.99	36.50	55.35	4.585	91.99	1.0916	1.1296
19	10	2.67	36.60	57.10	4.598	95.01	1.0978	1.1412
20	10	2.76	36.60	57.30	4.598	95.36	1.0986	1.1371
21	10	2.77	22.60	57.50	4.561	96.05	1.1000	1.1364
22	10	2.69	54.50	57.00	4.542	95.33	1.0985	1.1354
23	10	2.35	31.45	56.60	3.951	99.84	1.1078	1.1511
24	10	3.16	41.60	56.80	5.233	88.84	1.0851	1.1277
25	10	2.90	36.50	41.55	4.580	67.35	1.0406	1.0673
26	10	2.66	36.50	72.75	4.591	123.04	1.1558	1.1791
27	10	2.76	36.50	57.25	4.591	95.33	1.0985	1.1097
28	10	2.75	36.60	57.15	4.598	95.10	1.0980	1.1305
29	10	2.72	36.60	57.35	4.604	95.40	1.0986	1.1218

Note: Placebo normal stress model (Eq. (1)) is used to predict normal stress P2 at the roller compaction settings used to make active batches. Once P2 is estimated, placebo ribbon density model (Eq. (2)) is used to estimate ribbon densities.

3.8. Effect of de-aeration on normal stress measurements and gap

Alexanderwerk WP120 is equipped with vacuum pump for de-aeration of pre-blend. De–aeration of blend enhances consolidation of powder prior to its entry in nip region. The air suction point is located near nip zone of the pre-blend. Vacuum pump pulls air from pre-blend as it enters nip zone. Miller (1997) have shown that vacuum de-aeration is important during roller compaction to reduce pre-blend leak that occurs due to powder slippage between individual particles and roll surface. Their research showed that vacuum de-aeration decreased powder leakage significantly.

As the roller compaction progresses, the vacuum filter gets clogged, especially during longer runs. The rate of air mass transfer from the pre-blend to the vacuum pump decreases. If the vacuum pump cannot extract air from pre-blend prior to entering nip zone, it could impact ribbon properties. Therefore, in this experiment we have simulated filter clogging by varying vacuum pump capacity setting and studied its impact on normal stress measurements.

The placebo pre-blend was roller compacted at 8 rpm roll speed; 37 rpm screw speed, and 55 bar hydraulic roll pressure. Effects of vacuum levels on normal stress and gap are shown in Table 17.

Typically ΔP values for clean filter are ~750 mbar before starting the run. As can be seen from Table 17, during the roller compaction, at vacuum settings of ΔP = 460 mbar and ΔP = 160 mbar, the normal stress P2 and gap readings remained unchanged. However, when vacuum was turned off (i.e. $\Delta P \sim 0$ mbar), gap reading decreased to ~1.86 mm and normal stress P2 increased to ~128.2 MPa.

By turning vacuum off completely, de-aeration is absent. Due to presence of excess air in the pre-blend, net mass flow decreased due to poor grip between pre-blend and roll surface, resulting in decreased gap. As the gap decreased, normal stress P2 increased (at fixed hydraulic roll pressure of ~55 bar). These results are consistent with findings shown in Fig. 4 (Section 3.1) where decrease in screw speed to roll speed ratio (SR), (i.e. decrease in gap), resulted in increase in normal stress P2. No effect of vacuum level on normal stress for placebo pre-blend means vacuum pump is able to de-aerate the pre–blend despite being clogged.

Table 16
Root mean square errors (RMSE) and %RSD of data sets (3–5, 3–10, and 3–17%, w/w active blends).

Data set	Active blend concentration range (%, w/w)	Average compressibility factor	Average effective angle of friction (rad)	RMSE	%RSD
Set 1	3–17	5.134	0.6859	0.03614	3.20
Set 2	3–10	4.924	0.6652	0.02692	2.39
Set 3	3–5	4.664	0.6421	0.01398	1.24
Placebo	0	4.315	0.6181	0.01810	1.65

(1) The average value of compressibility and internal angle of friction for each set was calculated using corresponding data points from each set. For example, average value of compressibility and internal angle of friction for set 3 was calculated using all active blends with 3–5% (w/w) active concentrations (i.e. blends C, D, and E in Table 12). (2) For the calculation of RMSE and corresponding % RSD of each set, all the data points corresponding to active concentrations range (Table 15 – model predicted vs. experimental)) were used.

Table 17
Effect of vacuum on gap and measured normal stress (P2).

ΔP (mbar)	Gap (mm)	Screw speed (rpm)	Hydraulic roll pressure (bar)	Roll speed (rpm)	Normal stress P2 (MPa)
160	2.48	36.60	56.40	7.94	101.40
460	2.46	36.60	56.50	7.94	99.70
0(i.e. no vacuum)	1.86	36.70	57.70	7.94	128.20

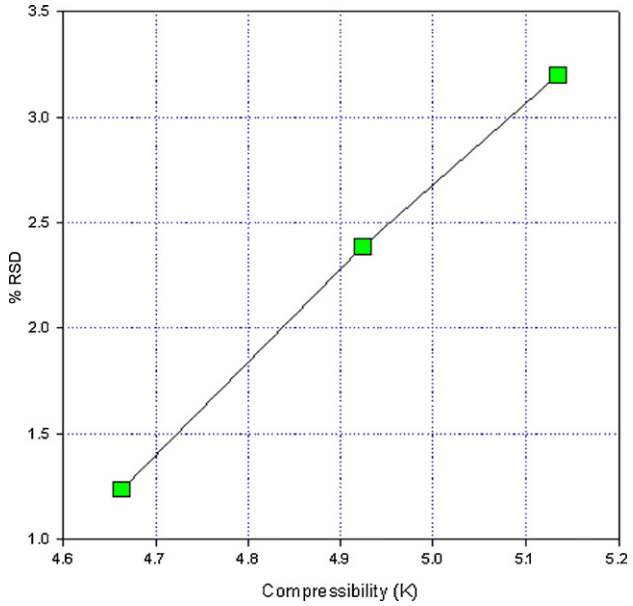

Fig. 14. %RSD as a Function of compressibility (K) for the active blends ribbon density predictions using placebo model. (Compressibility of placebo blend = 4.31.)

Additional studies using pre-blends with wide range of cohesivity may be necessary to study the effect of vacuum levels on normal stress measurements. For example, it is possible that vacuum level may be important for highly cohesive pre-blend. During roller compaction, vacuum filter clogs as the run progresses. The clogging of a vacuum filter reduces ΔP. For the highly cohesive pre-blends, the reduction in vacuum gradient means poor de-aeration and may impact ribbon density due to changes in normal stress on ribbon. The instrumented roll can be useful in determining the sensitivity of pre–blend de-aeration to vacuum level by studying effect of vacuum level on normal stress applied on ribbon. If we see changes in normal stress measurements at various levels of vacuum, it may indicate that pre-blend may be sensitive to vacuum filter clogging. In such cases, it may be necessary to change vacuum filter periodically, depending on batch size.

4. Conclusions

Application of instrumented roll technology for the process development of low drug formulations was successfully demonstrated using placebo and active formulations. This was achieved by designing an instrumented roll on WP120 roller compactor equipped with three pressure transducers. Instrumented roll provided normal stress applied on ribbon during roller compaction process in real time. Normal stress P2 was used for data analysis and it correlated well with process parameters such as roll speed, screw to roll speed ratio, and hydraulic roll pressure for both placebo and active formulations. Ribbon density of placebo formulation was mainly function of normal stress P2. Ribbon density of active formulations was function of normal stress P2 and gap.

Statistical models were developed using placebo and active pre-blends to express ribbon density as a function of maximum normal stress and gap in order to remove machine specific parameter dependence. Dec et al. (2003) have developed model relating basic properties of the feed material, roller press design and its operating parameters using finite element methods. The finite element method uses input about powder properties, roll and feed screw geometry and frictional conditions. However, use of these models can be complicated and require operator skills as compared to simpler statistical models developed and presented in this body of work.

The porosity vs. compaction pressure data of pre-blends used in conjunction with normal stress data from instrumented roll for each run were able to predict average ribbon density and compared well with experimentally measured ribbon density. Density–pressure equations for a given pre-blend can be included in AIM software to display on line ribbon density data during roller compaction runs. This approach can be used as another Process Analytical Tool technique in addition to on-line NIR ribbon density measurements.

Effect of blend properties (e.g. compressibility, compactibility) on normal stress measurements were evaluated by varying active ingredient and lubricant concentrations in active pre blends. Ribbon densities of active formulations calculated using placebo models compared well with experimentally measured values of active formulations. The %RSD of the prediction of active ribbon density using placebo model decreased as the % drug load of active formulations decreased. Effective angle of internal friction and compressibility (K) properties of active pre-blend may be used as key indicators for predicting ribbon densities of low drug load active blend using placebo ribbon density model.

For the process development of low drug load active blends, placebo models developed using instrumented roll can help reduce size of design of experiments provided effective angle of friction and compressibility (K) properties of active blends are comparable to that of the placebo blend. This approach will also help reduce consumption of valuable active drug substances during development and scale up work.

If a sufficient numbers of compounds are evaluated using limited DOE runs on instrumented roll, one may be able to use statistical models developed using pooled data to reduce size of design of experiments for a new active blend with high drug load, provided effective angle of friction and compressibility (K) properties of active blend are within the range studied. Additional studies with different active blends and varying drug loads will be needed to confirm this strategy.

The instrumented roll can be useful to study the effect of vacuum level on normal stress applied on ribbon. Using normal stress measurements of a pre-blend as a function of vacuum level, one can evaluate the sensitivity of pre-blend to vacuum filter clogging.

The current study was conducted using WP120 roller compactor which is a pilot scale machine. Efforts are ongoing to apply the findings from this study to scale up to commercial scale WP200 roller compactor. Data analysis using modified Johanson model with emphasis on scale up is in progress and will be a part of follow up paper (in preparation).

Acknowledgements

The authors would like to express their gratitude to Dr. Elena Zour for supporting the instrumented roll project. The authors

would also like to thank Dr. James Bergum for assistance in design of experiments, Brian Breza for pilot plant support, Gary Kovacs, Alexander Mbay for samples testing support, Kevin Macias and Anthony Tantuccio for shear cell analysis. Finally, contributions of Sam Dukler, Lev Tsygan, Sean Murphy (Metropolitan Computing Corporation, East Hanover, New Jersey) for the manufacture of instrumented roll system, and Sean Koontz (Alexanderwerk, Horsham, Pennsylvania) for data acquisition system modifications on WP120 roller compactor to communicate with instrumented roll system are greatly appreciated.

References

Bindhumadhavan, G., Seville, J.P.K., Adams, M.J., Greenwood, R.W., Fitzpatrick, S., 2005. Roll compaction of a pharmaceutical excipient: Experimental validation of rolling theory for granular solids. Chem. Eng. Sci. 60, 3891–3897.

Dec, R., Zavaliangos, A., Cunningham, J., 2003. Powder Technol. 130, 265–271.

Guigon, P., Simon, O., 2003. Roll press design – influence of force feed systems on compaction. Powder Tech. 130, 41–48.

Gupta, A., Garnet, P., Miller, R., Morris, K., 2005. Real-time near-infrared monitoring of content uniformity, moisture content, compact density, tensile strength, and young's modulus of roller compacted powder blends. J. Pharm. Sci. 94, 1589–1597.

Herting, M., Kleinebudde, P., 2007. Roll compaction/dry granulation: effect of raw material particle size on granule and tablet properties. Int. J. Pharm. 338, 110–118.

He, X., Secreast, P.J., Amidon, G.E., 2007. Mechanistic study of the effect of roller compaction and lubricant on tablet mechanical strength. J. Pharm. Sci. 96, 1342–1355.

Inghelbrecht, S., Remon, J., 1998. The roller compaction of different types of lactose. Int. J. Pharm. 166, 135–144.

Johanson, J.R., 1965. A rolling theory of granular solids. ASME, J. Appl. Mech. Ser. E 32 (4), 842–848.

Lee, T., Hsu, F., 2007. A cross-performance relationship between Carr's Index and dissolution rate constant. The study of acetaminophen batches. Drug Dev. Ind. Pharm. 33, 1273–1284.

Meyer, R., Roland, E., Cunningham, J., 2005. A parametric study of the effects of roller compaction process parameters on normal and shear stress distributions using an instrumented compaction roller. AAPS Annual Meeting Poster. AAPS J. 7 (S2).

Miller, R.W., 1997. Roller compaction technology. In: Parikh, D.M. (Ed.), Handbook of Pharmaceutical Granulation Technology. Marcel Dekker, New York, pp. 99–150.

Moguelez-Moran, A.M., Wu, C.Y., Seville, J.P.K., 2008. The effect of lubrication on density distributions of roller compacted ribbons. Int. J. Pharm. 362, 52–59.

Simon, O., Guigon, P., 2003. Correlation between powder-packing properties and roll press compact heterogeneity. Powder Tech. 130, 257–264.

Zinchuk, A.V., Mullarney, M.P., Hancock, B.C., 2004. Simulation of roller compaction using a laboratory scale compaction simulator. Int. J. Pharm. 269, 403–415.